ACS APPLIED MATERIALS & INTERFACES

Research Article

www.acsami.org

Solution-Processed Barium Salts as Charge Injection Layers for High Performance N-Channel Organic Field-Effect Transistors

Nam-Koo Kim,[†] Dongyoon Khim,[†] Yong Xu,[‡] Seung-Hoon Lee,[†] Minji Kang,[†] Jihong Kim,[†] Antonio Facchetti,[§] Yong-Young Noh,*[,‡] and Dong-Yu Kim*[,†]

[†]Department of Nanobio Materials and Electronics, School of Material Science and Engineering, Heeger Center for Advanced Materials, Gwangju Institute of Science and Technology (GIST), 261 Cheomdan-gwagiro (Oryong-dong), Buk-gu, Gwangju 500-712, Republic of Korea

[‡]Department of Energy and Materials Engineering, Dongguk University, 26 Pil-dong, 3-ga, Jung-gu, Seoul 100-715, Republic of Korea

[§]Polyera Corporation, 8045 Lamon Avenue, Skokie, Illinois 60077, United States

ABSTRACT: N-channel organic field-effect transistors (OFETs) have generally shown lower field-effect mobilities (μ_{FET}) than their p-type counterparts. One of the reasons is the energetic misalignment between the work function (WF) of commonly used charge injection electrode, i.e. gold (Au), and the lowest unoccupied molecular orbital (LUMO) of n-channel electron-transporting organic semiconductors. Here, we report barium salts as solution-processed interlayers, to improve the electron-injection and/or hole-blocking in top-gate/bottom-contact n-channel OFETs, based on poly{[*N*,*N*′-bis(2-octyldodecyl)-naphthalene-1,4,5,8-bis(dicarboximide)-2,6-diyl]-*alt*-5,5′-(2,2′-dithiophene)} (P(NDI2OD-T2)) and phenyl-C61-butyric acid methyl ester ($PC_{61}BM$). Two different barium salts, barium hydroxide ($Ba(OH)_2$) and barium chloride ($Ba(Cl)_2$), are employed as the ultrathin interlayer (~2 nm); and they effectively tune the WF of Au from 4.9 eV, to as low as 3.5 eV. The resulting n-channel OFETs exhibit significantly improved μ_{FET}, approaching 2.6 $cm^2/(V\ s)$ and 0.1 $cm^2/(V\ s)$ for the best P(NDI2OD-T2) and $PC_{61}BM$ devices, respectively, with $Ba(OH)_2$ as interlayer.

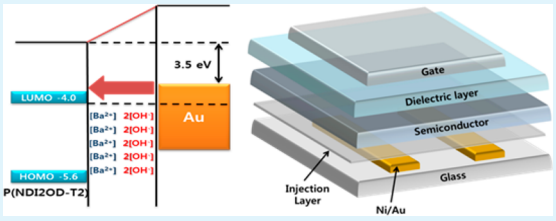

KEYWORDS: *organic field-effect transistor, charge injection, interlayer, barium salts, work function*

INTRODUCTION

During the past 20 years, organic field-effect transistors (OFETs) have been actively pursued for applications and fabrication methodologies that are complementary to those of conventional inorganic transistors.[1−3] Among them, solution processability of the FET stack provides a new paradigm in device manufacturing, through the cost-effective graphic art printing process.[4−6] State-of-the-art solution processed *p*-type OFETs show impressively high field-effect mobility (μ_{FET}) of over 10 $cm^2/(V\ s)$, which is mainly achieved via the synthesis/development of new organic semiconductors (OSCs) and gate dielectric materials, as well as improvement of the semiconductor molecular orientation, alignment, and thin-film crystallinity.[7−9] However, the performance of n-channel OFETs remains lower than their p-type counterparts, because of several major restrictions. One of them is the generation of a large number of electron trapping sites within the semiconductor bandgap, by chemical functionalities on the dielectric surface, such as hydroxyl groups, or water and oxygen from the ambient atmosphere.[10,11] These drawbacks can be overcome by using hydroxyl-free polymer dielectric materials, such as a divinyl tetramethylsiloxane-bis(benzocyclobutene) derivative, or an efficient encapsulation of the device.[11−13] The other restriction is the poor electron injection properties, due to the energetic misalignment between the lowest unoccupied molecular orbital (LUMO) energetic level of n-channel OSCs, and the work function (WF) of the common contact metal used in OFETs, i.e. Au. Generally, high WF metals such as Au and Ti are used as the contact electrode, due to their high ambient stability, and photo pattern-ability. However, the LUMO energy level of typical n-channel OSCs are located far away from the WF of stable metal electrodes, leading to a large injection barrier height.[14,15] Therefore, several approaches to improve charge injection properties in n-channel OFETs have been reported.

The conventional approach to overcoming the above limitations is by utilizing low WF metals, such as Al and Ca, as an electron injection electrode; typically, they showed better charge injection properties than Au.[16,17] However, these metals are easily prone to oxidation in air, and during photolithography processes for source/drain patterning. An alternative method is by inserting various interlayers[17−22] at the metal/OSC interface, in order to shift the WF of the contact metal, by means of chemical/charge transfer, and/or dipole formation. In general, deposition of electron injection layers on the contact surface by thermal evaporation or solution processes, such as conjugated polyelectrolytes, nonconjugated polyelectrolytes, and metal oxides, is compatible with various

Received: April 3, 2014
Accepted: June 3, 2014
Published: June 3, 2014

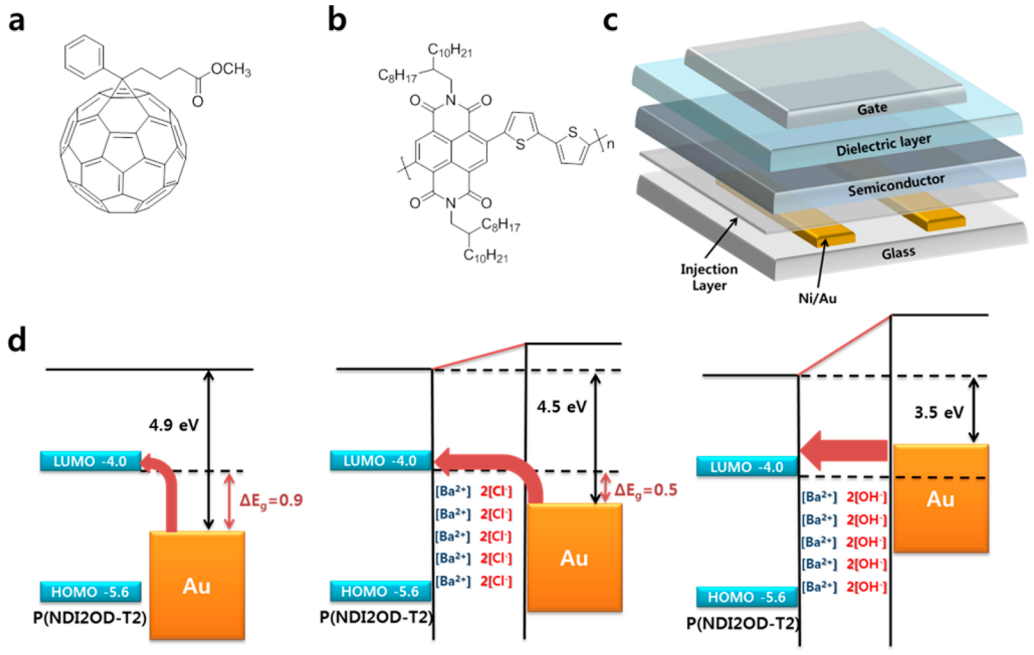

Figure 1. (a) Molecular structure of $PC_{61}BM$, and (b) P(NDI2OD-T2); (c) TG/BC OFET device structure with interfacial layer; (d) energy diagram of P(NDI2OD-T2) on pristine Au S/D electrode, and after incorporation of the $Ba(OH)_2$ and $Ba(Cl)_2$, between the P(NDI2OD-T2) and Au.

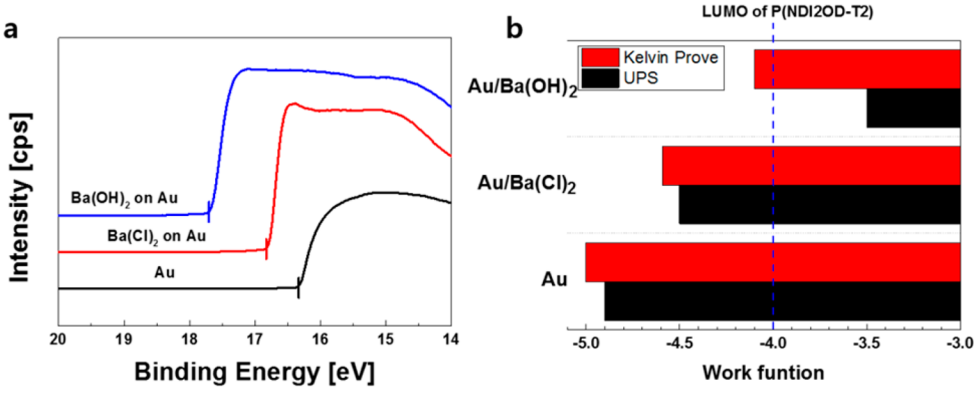

Figure 2. (a) Ultraviolet photoemission spectra (UPS) of different barium interfacial layer on an Au contact. (b) Work function of an Au with and without barium interfacial layer, as independently measured by Kelvin probe in air, and by UPS.

kinds of electrode material. Several inorganic salts have also been pursued as electron injection interlayers in various organic electronic devices, where WF reduction of the metal contacts enhanced performance.[23−26] Among these treatments, a double layer of barium hydroxide and zinc oxide has previously been utilized as an electron-injection interlayer in polymer light emitting diodes, and the resulting devices showed better charge balance between holes and electrons, and much reduced exciton quenching.[27] Therefore, a single layer of barium salts alone could be another good candidate for electron-injecting material in n-channel OFETs. In addition, it can be easily deposited by solution-based processing, and it is commercially available at very low cost.

Here we report two solution-processed barium salts, barium hydroxide ($Ba(OH)_2$) and barium chloride ($Ba(Cl)_2$), as electron-injection interlayers between the Au electrodes and the OSC, in top-gate/bottom-contact (TG/BC) n-channel OFETs. Our results demonstrate significantly improved charge injection efficiency (2−10× reduction in contact resistance), and greatly enhanced device performance (3−5× increase in electron mobility). To elucidate these remarkable improvements, we systematically investigated the physical and chemical properties of the electrical contact metal surface and the contact-OSC interface, by using various tools, including atomic force microscopy (AFM), Kelvin probe, UV photoelectron spectroscopy (UPS), and X-ray photoelectron spectroscopy (XPS).

RESULTS AND DISCUSSION

Two representative n-channel organic semiconductors, the small molecule phenyl-C61-butyric acid methylester ($PC_{61}BM$) and the polymer poly{[*N*,*N*′-bis(2-octyldodecyl)-naphthalene-1,4,5,8-bis(dicarboximide)-2,6-diyl]-*alt*-5,5′-(2,2′-dithiophene)} (P(NDI2OD-T2)), were used in this study, and their chemical structures are shown in panels a and b in Figure 1, respectively. $PC_{61}BM$ and P(NDI2OD-T2) are widely used in organic electronics, and their HOMO and LUMO levels are 6.1 and 3.7 eV for $PC_{61}BM$, and 5.6 and 4.0 eV for P(NDI2OD-T2),

dx.doi.org/10.1021/am502007j | ACS Appl. Mater. Interfaces 2014, 6, 9614−9621

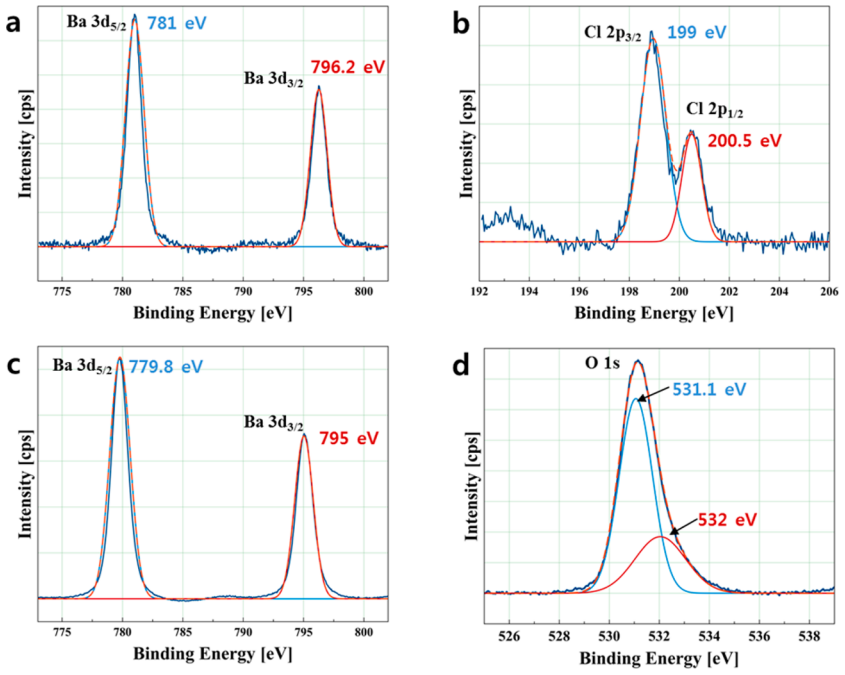

Figure 3. X-ray photoemission spectra of the spin-coated $Ba(Cl)_2$ and $Ba(OH)_2$ films on Au contacts. (a) Ba 3d spectra, and (b) Cl 2p spectra of $Ba(Cl)_2$ films. (c) Ba 3d spectra, and (d) O 1s spectra of $Ba(OH)_2$ films, respectively.

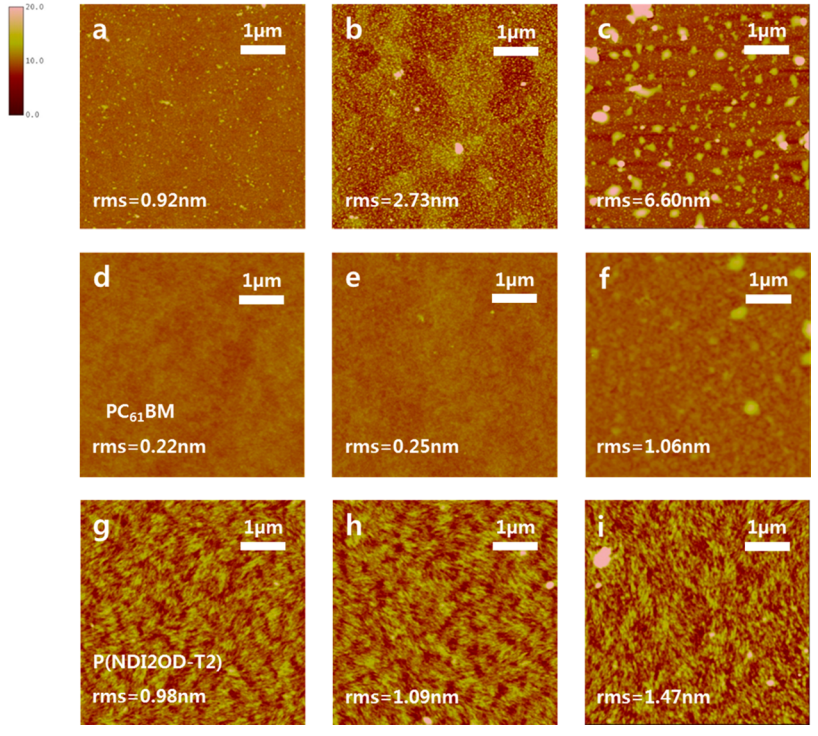

Figure 4. Tapping mode AFM images. (a) Bare Au surface, and with (b) $Ba(OH)_2$-coated and (c) $Ba(Cl)_2$-coated Au surface. $PC_{61}BM$ films were coated onto (d) bare Au, and with (e) $Ba(OH)_2$/Au, and (f) $Ba(Cl)_2$/Au; and (g) P(NDI2OD-T2) on Au contact, and with (h) $Ba(OH)_2$/Au, and (i) $Ba(Cl)_2$/Au surface (rms: root-mean-square roughness).

respectively.[12,28,29] The charge transport properties of these two materials were measured using top-gate/bottom-contact (TG/BC) OFETs fabricated on glass substrates, with Au source/drain contacts. $Ba(OH)_2$ or $Ba(Cl)_2$ solutions were optionally spin-coated as an electron-injection interlayer (see Figure 1c). A spin-coated semiconductor layer, and subsequently a dielectric poly(methyl methacrylate) (PMMA) layer, were deposited on top of the barium salt; and the OFET devices were completed by thermal evaporation of an aluminum (Al) top-gate electrode (see Experimental Section for details).

Figure 2 show UPS and Kelvin probe results of pristine Au, as well as $Ba(OH)_2$ and $Ba(Cl)_2$ thin film on Au/glass substrates. Small discrepancy between UPS and Kelvin probe

dx.doi.org/10.1021/am502007j | ACS Appl. Mater. Interfaces 2014, 6, 9614−9621

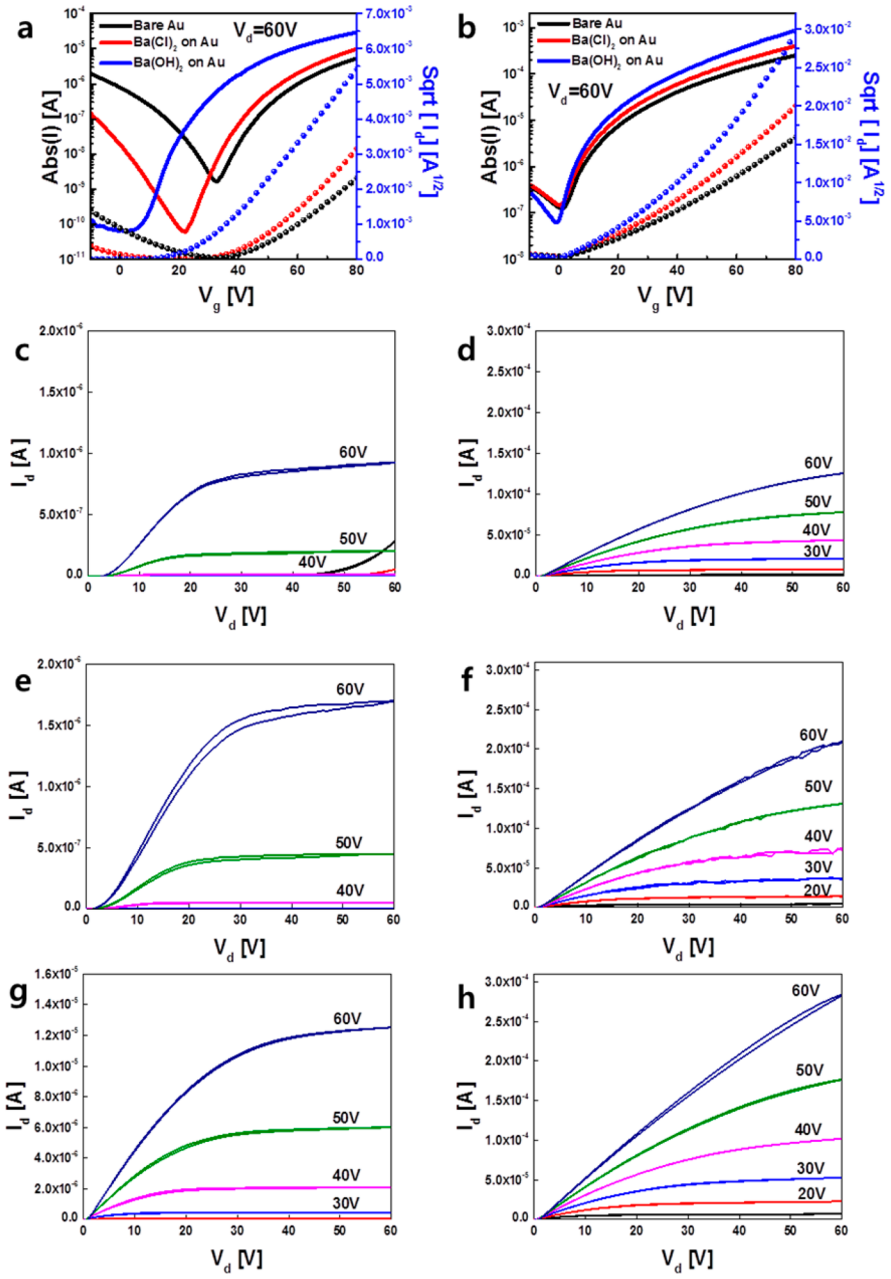

Figure 5. Transfer curve characteristics of the n-channel OFETs (W/L = 1 mm/20 μm) based on (a) $PC_{61}BM$, and (b) P(NDI2OD-T2), with and without $Ba(Cl)_2$ and $Ba(OH)_2$ interfacial layers. Output characteristics of the n-channel OFETs based on (c) $PC_{61}BM$ on Au contact, and on (e) $Ba(Cl)_2$/Au, and (g) $Ba(OH)_2$/Au; and (d) P(NDI2OD-T2) on Au contact, and with (f) $Ba(Cl)_2$/Au, and (h) $Ba(OH)_2$/Au, at V_g = 10, 20, 30, 40, 50, and 60 V.

results are due to different measurement environments, instruments and sensitivity.[30] Both measurements indicate that barium salts do indeed strongly reduce the WF of the Au electrodes, and that the magnitude of WF shift depends on the barium salt materials. The WF of Au was reduced from 4.9 to 4.4 and 3.5 eV, with $Ba(Cl)_2$ and $Ba(OH)_2$ interlayer, respectively. Thanks to this noticeable reduction of Au WF, electrons should be much more easily injected into the LUMO levels of our semiconductors, which are located at 3.7 eV for $PC_{61}BM$, and 4.0 eV for P(NDI2OD-T2). The shift of Au WF is presumably due to dipole formation on the Au surface; thus the degree of shifting can be influenced by the intrinsic magnitude of these salt dipole moments,[20,31] the degree of coverage on Au, and the morphology of the interlayer film.

The chemical nature and surface morphology of $Ba(OH)_2$ and $Ba(Cl)_2$ ultrathin films (2−3 nm) were accessed by X-ray photoemission spectroscope (XPS) and atomic force microscope (AFM) measurements. The XPS spectra were calibrated using adventitious carbon fixation at the binding energy of 285 eV, to compensate for the charge effects. Figure 3 shows the XPS profiles of the Ba 3d, Cl 2p, and O 1s of $Ba(OH)_2$ and $Ba(Cl)_2$, indicating that both $Ba(OH)_2$ and $Ba(Cl)_2$ interlayers do not react with the metal electrode. As shown in Figure 3d, the oxygen signal at EB(O $1s_A$) ≈ 531.1 eV corresponds to the hydroxide ions of the $Ba(OH)_2$ layer; and the peak at EB(O $1s_B$) ≈ 532 eV could be attributed either to the oxidation states of Au, or to surface contamination.[32,33] The AFM images shown in Figure 4 reveal that the surfaces of $Ba(OH)_2$ and

dx.doi.org/10.1021/am502007j | ACS Appl. Mater. Interfaces 2014, 6, 9614−9621

Table 1. OFET Parameters of the $PC_{61}BM$ and P(NDI2OD-T2) Devices, with Different Barium Salt Interfacial Layers

OSC	interfacial layer	μ_e (cm^2/(V s))	V_{Th} (V)	$S_{S\text{-}th}$ (V/dec.)	I_{on}/I_{off}	R_c (Ω cm)
$PC_{61}BM$	none	0.034 (± 0.001) (max 0.036)	45.19 (± 1.56)	6.38 (± 0.26)	3×10^3	1.3×10^6
	$Ba(Cl)_2$	0.062 (± 0.004) (max 0.07)	48.20 (± 1.68)	4.97 (± 0.23)	2×10^5	8.3×10^5
	$Ba(OH)_2$	0.094 (± 0.009) (max 0.101)	28.59 (± 0.62)	4.59 (± 0.72)	4×10^5	6.6×10^4
P(NDI2OD-T2)	none	0.37 (± 0.07) (max 0.44)	16.86 (± 1.42)	7.34 (± 1.08)	10^3	3.6×10^3
	$Ba(Cl)_2$	0.79 (± 0.13) (max 0.98)	20.98 (± 1.60)	6.08 (± 0.57)	3×10^3	1.1×10^3
	$Ba(OH)_2$	1.54 (± 0.54) (max 2.57)	26.81 (± 4.67)	4.51 (± 1.22)	10^4	5.3×10^2

[a]The electron mobility (μ_e) and the threshold voltage (V_{Th}) were calculated at the saturation region (V_d = 60 V), using gradual channel approximation equations (W/L = 1.0 mm/20 μm), whereas PMMA gate dielectric thickness and capacitance were ~500 nm and ~6.2 nF/cm^2, and CYTOP, ~350 nm and ~5.3 nF/cm^2, respectively. Contact resistance (R_c) was obtained using the transfer-length method (V_d = 60 V).

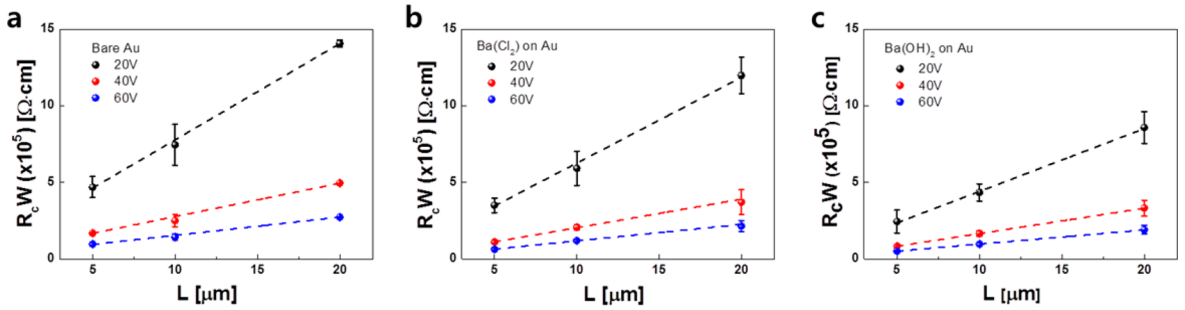

Figure 6. Channel width (W) normalized n-channel contact resistance (R_cW) of the (a) P(NDI2OD-T2) OFETs, with (b) $Ba(Cl)_2$, and (c) $Ba(OH)_2$ interfacial layers.

$Ba(Cl)_2$ thin films exhibit different morphology on Au. Both surfaces showed aggregated nanosized dots, but the $Ba(OH)_2$ surface showed much smaller sized dots, with a larger coverage than the $Ba(Cl)_2$. The reduced surface coverage of $Ba(Cl)_2$ can partially explain the smaller WF shift of $Ba(Cl)_2$ deposited Au electrode. Despite the different morphologies of these interlayers, the morphology of subsequently deposited OSC film is not affected by the underlying surface topology. The AFM images in Figure 4d–i show that all $PC_{61}BM$ films exhibit smooth surface morphology and all P(NDI2OD-T2) films always exhibit a highly ordered fiber-like morphology, independent of the underlying surface. Because the channel in top-gate OFETs is situated on the top surface of OSC film, the transistor characteristics are not greatly influenced by the underneath interlayers, as long as a chemical reaction does not occur, as in this case; and thus, the film morphology is unaffected.

Panels a and b in Figure 5 show the transfer characteristics of $PC_{61}BM$ and P(NDI2OD-T2) OFETs on bare Au, $Ba(Cl)_2$/Au, and $Ba(OH)_2$/Au contact. The untreated $PC_{61}BM$ devices showed typical V-shape ambipolar transfer characteristics, with a field-effect electron mobility (μ_e), threshold voltage (V_{th}), on/off ratio (I_{on}/I_{off}), and a hole mobility (μ_h) of 0.034, +45.2 V, 3×10^3, and 0.017 cm^2/(V s), respectively. The small reduction (from 4.9 to 4.4 eV) of Au WF with $Ba(Cl)_2$ interlayer changes the balanced ambipolar characteristics to be n-channel dominant characteristics, with μ_e = 0.062 cm^2/(V s), V_{th} = 48.20 V, $I_{on}/I_{off} = 2 \times 10^5$, and μ_h < 0.005 cm^2/(V s). The larger WF shift (from 4.9 to 3.5 eV) by using $Ba(OH)_2$ leads to nearly unipolar n-channel characteristics, with μ_e = 0.094 cm^2/(V s) and a higher $I_{on}/I_{off} = 4 \times 10^5$, due to the much reduced injection barrier for electrons, and elevated barrier to holes. Enhanced n-channel performances are also observed in the output characteristics of Figure 5c, e, and g. The sublinearity at small drain voltage of the bare Au device is clearly alleviated by inserting a barium salts based interlayer, indicating a transition from Schottky, to Ohmic-like contacts. In particular, $PC_{61}BM$ OFETs with $Ba(OH)_2$ interlayer showed more improved device characteristics, than those with $Ba(Cl)_2$. Similar improvement by barium salt-based interlayers are observed for the OFETs with the polymeric semiconductor P(NDI2OD-T2). Typical P(NDI2OD-T2) OFETs have exhibited μ_e of 0.1–1 cm^2/(V s) in ambient conditions, with several polymeric dielectrics and Au contacts.[34−36] Our control P(NDI2OD-T2) OFETs with bare Au contacts also showed comparable μ_e of 0.37 cm^2/(V s) (max 0.44 cm^2/(V s)). The μ_e of P(NDI2OD-T2) OFETs significantly increases to 0.79 cm^2/(V s) (max = 0.98 cm^2/(V s)) and 1.57 cm^2/(V s) (max = 2.57 cm^2/(V s)), by inserting $BaCl_2$ and $Ba(OH)_2$ interlayers, respectively. All of the OFET parameters are summarized in Table 1. This is the highest μ_e value reported so far for naphthalene diimide (NDI)-based polymer OFETs. The reported highest μ_e for P(NDI2OD-T2) OFETs was 1 cm^2/(V s), and other NDI derivatives exhibited a maximum μ_e of 1.8 cm^2/(V s).[37,38] These performances approach those of the best n-channel OSCs, with very few exceptions, at (~2–4 cm^2/(V s)).[39−44] Thus, these results can potentially enable the fabrication of balanced p- and n-channel OFETs, for complementary integrated circuits.[45,46]

With constant device miniaturization for high-speed operation and high-density integration, the contact resistance (R_c) is becoming greater than the channel resistance. For OFETs, this is closely related to the charge-injection properties between the S/D electrodes and the OSC.[47] The channel-width normalized contact resistance (R_cW) for our P(NDI2OD-T2)-based OFETs were extracted using the transfer-length method (TLM) for quantitative exploration of the charge injection efficiency, and thus rationalization of the observed OFET performance.[48] Figure 6 shows that the total resistance, including the contributions of the channel and the contact resistance, is proportional to the channel length (L); thus the R_c can be obtained from the intercept on the Y-axis, by performing a linear regression of $R_{tot}W$ versus L. The R_cW of

dx.doi.org/10.1021/am502007j | ACS Appl. Mater. Interfaces 2014, 6, 9614–9621

P(NDI2OD-T2) OFETs with bare Au contacts is found to be 3.6×10^3 Ω cm, a value comparable to the data reported in the literature.[35,49] Importantly, these values are considerably reduced to 1.1×10^3 and 5.3×10^2 Ω cm, by using $Ba(Cl)_2$ and $Ba(OH)_2$ as interlayers, respectively. The R_c reduction confirms that our devices were contact-limited, corroborating the effect of using the barium salts as interlayers.

CONCLUSION

We demonstrated high-performance n-channel OFETs, by using an ultrathin electron-injection interlayer, based on barium salts. By inserting $Ba(OH)_2$ and $Ba(Cl)_2$ thin films between the Au S/D electrodes and the OSCs, via a simple spin coating process, the performance of the corresponding TG/BC $PC_{61}BM$ and P(NDI2OD-T2) OFETs were dramatically improved. $PC_{61}BM$ and P(NDI2OD-T2) OFETs exhibit the highest μ_e of ~0.10 and ~2.6 $cm^2/(V\ s)$, which are 3−5 times higher than the initial values of 0.034 and 0.37 $cm^2/(V\ s)$, respectively. UPS, XPS, and AFM results showed that the WF of Au electrodes is reduced by insertion of the barium salt interlayers, through the formation of molecular dipoles. The degree of WF shift depended on the surface coverage, and the magnitude of the dipole moment of the interlayer. This study indicates that the electron injection property is one of the critical limitations to achieving high μ_e in n-channel OFETs; and that solution-processed barium salts can be an effective interlayer to control the contact properties, to realize high-performance n-channel OFETs and complementary integrated circuits.

EXPERIMENTAL METHODS

Field-Effect Transistor Fabrication. Corning Eagle 2000 glass substrates were cleaned sequentially in an ultrasonic bath, with deionized water, acetone, and isopropanol, for 10 min each. The Au/Ni (12 nm/3 nm thick) patterns for source and drain electrodes were fabricated using conventional photolithography. $Ba(OH_2)$ and $Ba(Cl_2)$ were purchased from Aldrich, and dissolved in methanol for use (2 mg/mL concentration). The charge injection layers ($Ba(OH_2)$, $Ba(Cl_2)$) were deposited by spin-coating at 4000 rpm under N_2 condition, onto the Au patterned electrodes, over substrates. The n-channel semiconducting material, P(NDI2OD-T2), was purchased from Polyera Corporation; and $PC_{61}BM$ was purchased from Nano-C, and used as received. P(NDI2OD-T2) and $PC_{61}BM$ were dissolved in anhydrous chlorobenzene to obtain 10 mg/mL solutions, and were then each spin-coated at 2000 rpm, in a N_2-purged glovebox. Each solution was filtered with a 0.45 μm polytetrafluoroethylene (PTFE) syringe filter, before spin coating. The P(NDI2OD-T2) polymers and the $PC_{61}BM$ films were thermally annealed at 200 and 110 °C for 20 min, respectively, to remove the residual solvents, and induce an ordered crystalline phase, in a glovebox with N_2 atmosphere. PMMA (Aldrich, M_w = 120 kDa) and CYTOP (Asahi Glass) were used as dielectric materials, without further purification. PMMA (80 mg/mL) was dissolved in *n*-butylacetate, and CYTOP was dissolved in CT-Solv.180 at 2:1 ratio, and the solution was filtered with a 0.45 μm PTFE syringe filter, before spin coating. After deposition, the devices were baked at 80 °C for 2 h, under N_2 conditions. Transistor fabrication was completed by deposition of aluminum top-gate electrode by thermal evaporation (~50 nm-thick), using metal shadow masks.

Thin Film and Device Characterizations. The surface morphology of barium salts was investigated by tapping-mode AFM (Nanoscope III, Veeco Instruments, Inc.). The contact potential difference of each sample was detected by Kelvin probe (KP 6500 Digital Kelvin probe, McAllister Technical Service, Co. Ltd.), in air. The XPS and UPS measurements were carried out using AXIS-NOVA (Kratos, Inc.), with a base pressure of 4.2×10^{-9} Torr. The OFET electrical characteristics were measured using a semiconductor parameter analyzer (Keithley 4200-SCS), in N_2-filled glovebox. The field-effect mobility (μ_{FET}) and threshold voltage (V_{Th}) were calculated from the saturation regime, using equations for classical silicon MOSFETs.

AUTHOR INFORMATION

Corresponding Authors

*E-mail: yynoh@dongguk.edu.

*E-mail: kimdy@gist.ac.kr.

Notes

The authors declare no competing financial interest.

ACKNOWLEDGMENTS

This work was supported by a National Research Foundation of Korea (NRF) grant, funded by the Korea government (MSIP) (2013-059210, NRF-2009-C1AAA001-2009-0092950 and 2008-0062606, CELA-NCRC); by the Center for Advanced Soft-Electronics funded by the Ministry of Science, ICT and Future Planning as Global Frontier Project (2013M3A6A5073183); and by the Dongguk University Research Fund of 2014. We thank the Korea Basic Science Institute (KBSI), for AFM, UPS, and XPS measurements.

REFERENCES

(1) Sirringhaus, H. Organic Field-Effect Transistors: The Path Beyond Amorphous Silicon. *Adv. Mater.* **2014**, *26*, 1319−1335.

(2) Facchetti, A. π-Conjugated Polymers for Organic Electronics and Photovoltaic Cell Applications. *Chem. Mater.* **2011**, *23*, 733−758.

(3) Baeg, K.-J.; Caironi, M.; Noh, Y.-Y. Toward Printed Integrated Circuits based on Unipolar or Ambipolar Polymer Semiconductors. *Adv. Mater.* **2013**, *25*, 4210−4244.

(4) Natali, D.; Caironi, M. Charge Injection in Solution-Processed Organic Field-Effect Transistors: Physics, Models and Characterization Methods. *Adv. Mater.* **2012**, *24*, 1357−1387.

(5) Menard, E.; Meitl, M. A.; Sun, Y.; Park, J.-U.; Shir, D. J-L.; Nam, Y.-S.; Jeon, S.; Rogers, J. A. Micro- and Nanopatterning Techniques for Organic Electronic and Optoelectronic Systems. *Chem. Rev.* **2007**, *107*, 1117−1160.

(6) Noh, Y.-Y.; Zhao, N.; Caironi, M.; Sirringhaus, H. Downscaling of Self-aligned, All-printed Polymer Thin-film Transistors. *Nat. Nanotechnol.* **2007**, *2*, 784−789.

(7) Minemawari, H.; Yamada, T.; Matsui, H.; Tsutsumi, J.; Haas, S.; Chiba, R.; Kumai, R.; Hasegawa, T. Inkjet Printing of Single-crystal Films. *Nature* **2011**, *475*, 364−367.

(8) Diao, Y.; Tee, B. C-K.; Girl, G.; Xu, J.; Kim, D. H.; Becerril, H. A.; Stoltenberg, R. M.; Lee, T. H.; Xue, G.; Mannsfeld, S. C. B.; Bao, Z. Solution Coating of Large-area Organic Semiconductor Thin Films with Aligned Single-crystalline Domains. *Nat. Mater.* **2013**, *12*, 665−671.

(9) Tseng, H.-R.; Phan, H.; Luo, C.; Wang, M.; Perez, L. A.; Patel, S. N.; Ying, L.; Kramer, E. J.; Nguyen, T.-Q.; Bazan, G. C.; Heeger, A. J. High-Mobility Field-Effect Transistors Fabricated with Macroscopic Aligned Semiconducting Polymers. *Adv. Mater.* **2014**, *26*, 2993−2998.

(10) Nicolai, H. T.; Kuik, M.; Wetzelaer, G. A. H.; de Boer, B.; Campbell, C.; Risko, C.; Brédas, J. L.; Blom, P. W. M. Unification of Trap-limited Electron Transport in Semiconducting Polymers. *Nat. Mater.* **2012**, *11*, 882−887.

(11) Chua, L.-L.; Zaumseil, J.; Chang, J.-F.; Ou, E. C.-W.; Ho, P. K.-H.; Sirringhaus, H.; Friend, R. H. General Observation of N-type Field-effect Behaviour in Organic Semiconductors. *Nature* **2005**, *434*, 194−199.

(12) Wöbkenberg, P. H.; Bradley, D. D. C.; Kronholm, D.; Hummelen, J. C.; de Leeuw, D. M.; Cölle, M.; Anthopoulos, T. D. High Mobility n-Channel Organic Field-effect Transistors Based on Soluble C60 and C70 Fullerene Derivatives. *Synth. Met.* **2008**, *158*, 468−472.

(13) Singh, T. B.; Narjanović, N.; Stadler, P.; Auinger, M.; Matt, G. J.; Günes, S.; Sariciftci, N. S.; Schwödiauer, R.; Bauer, S. Fabrication and Characterization of Solution-processed Methanofullerene-based Organic Field-effect Transistors. *J. Appl. Phys.* **2005**, *97*, 083714.
(14) Braun, S.; Salaneck, W. R.; Fahlman, M. Energy-Level Alignment at Organic/Metal and Organic/Organic Interfaces. *Adv. Mater.* **2009**, *21*, 1450−1472.
(15) Osikowicz, W.; Jong, M. P.; Braun, S.; Tengstedt, C.; Fahlman, M.; Salaneck, W. R. Energetics at Au Top and Bottom Contacts on Conjugated Polymers. *Appl. Phys. Lett.* **2006**, *88*, 193504.
(16) Zaumseil, J.; Friend, R. H.; Sirringhaus, H. Spatial Control of the Recombination Zone in an Ambipolar Light-emitting Organic Transistor. *Nat. Mater.* **2006**, *5*, 69−74.
(17) Noh, Y.-Y.; Cheng, X.; Tell, M.; Lee, M.-J.; Sirringhaus, H. Controlling Contact Resistance in Top-gate Polythiophene-based Field-effect Transistors by Molecular Engineering. *Semicond. Sci. Technol.* **2011**, *26*, 034003.
(18) Cheng, X.; Noh, Y.-Y.; Wang, J.; Tello, M.; Frisch, J.; Blum, R.-P.; Vollmer, A.; Rabe, J. P.; Koch, N.; Sirringhaus, H. Controlling Electron and Hole Charge Injection in Ambipolar Organic Field-Effect Transistors by Self-Assembled Monolayers. *Adv. Funct. Mater.* **2009**, *19*, 2407−2415.
(19) Kim, S. H.; Lee, J. H.; Yang, Y. S.; Lee, J.-I.; Zyung, T. N-Type Organic Thin-Film Transistors with Self-Assembled Monolayers. *J. Korean Phys. Soc.* **2003**, *42*, 551−554.
(20) Zhou, Y.; Fuentes-Hernandez, C.; Shim, J.; Meyer, J.; Giordano, A. J.; Li, H.; Winget, P.; Papadopoulos, T.; Cheun, H.; Kim, J.; Fenoll, M.; Dindar, A.; Haske, W.; Najafabadi, E.; Khan, T. M.; Sojoudi, H.; Barlow, S.; Graham, S.; Brédas, J.-L.; Marder, S. R.; Kahn, A.; Kippelen, B. A Universal Method to Produce Low−Work Function Electrodes for Organic Electronics. *Science* **2012**, *336*, 327−332.
(21) Seo, J. H.; Gutacker, A.; Walker, B.; Cho, S.; Garcia, A.; Yang, R.; Nguyen, T.-Q.; Heeger, A. J.; Bazan, G. C. Improved Injection in n-Type Organic Transistors with Conjugated Polyelectrolytes. *J. Am. Chem. Soc.* **2009**, *131*, 18220−18221.
(22) Kang, H.; Hong, S.; Lee, J.; Lee, K. Electrostatically Self-Assembled Nonconjugated Polyelectrolytes as an Ideal Interfacial Layer for Inverted Polymer Solar Cells. *Adv. Mater.* **2012**, *24*, 3005−3009.
(23) Baeg, K.-J.; Kim, J.; Khim, D.; Caironi, M.; Kim, D.-Y.; You, I.-K.; Quinn, J. R.; Facchetti, A.; Noh, Y.-Y. Charge Injection Engineering of Ambipolar Field-Effect Transistors for High-Performance Organic Complementary Circuits. *ACS Appl. Mater. Interfaces* **2011**, *3*, 3205−3214.
(24) Brabec, C. J.; Shaheen, S. E.; Winder, C.; Sariciftci, N. S.; Denk, P. Effect of LiF/metal Electrodes on the Performance of Plastic Solar Cells. *Appl. Phys. Lett.* **2002**, *80*, 1288−1290.
(25) Hwang, J.; Xu, Z.; Yang, Y. Low-Work-Function Surface Formed by Solution-Processed and Thermally Deposited Nanoscale Layers of Cesium Carbonate. *Adv. Funct. Mater.* **2007**, *17*, 1966−1973.
(26) Khim, D.; Baeg, K.-J.; Kim, J.; Yeo, J.-S.; Kang, M.; Amegadzea, P. S. K.; Kim, M.-G.; Cho, J.; Lee, J. H.; Kim, D.-Y.; Noh, Y.-Y. Electron Injection Enhancement by a Cs-salt Interlayer in Ambipolar Organic Field-effect Transistors and Complementary Circuits. *J. Mater. Chem.* **2012**, *22*, 16979−16985.
(27) Lu, L. P.; Kabra, D.; Friend, R. H. Barium Hydroxide as an Interlayer Between Zinc Oxide and a Luminescent Conjugated Polymer for Light-Emitting Diodes. *Adv. Funct. Mater.* **2012**, *22*, 4165−4171.
(28) Anthopoulos, T. D.; de Leeuw, D. M.; Cantatore, E.; Setayesh, S.; Meijer, E. J.; Tanase, C.; Hummelen, C.; Blom, P. W. M. Organic Complementary-like Inverters Employing Methanofullerene-based Ambipolar Field-effect Transistors. *Appl. Phys. Lett.* **2004**, *85*, 4205−4207.
(29) Szendrei, K.; Jarzab, D.; Chen, Z.; Facchetti, A.; Loi, M. A. Ambipolar All-polymer Bulk Heterojunction Field-effect Transistors. *J. Mater. Chem.* **2010**, *20*, 1317−1321.
(30) Kim, J. S.; Lägel, B.; Moons, E.; Johansson, N.; Baikie, I. D.; Salaneck, W. R.; Fried, R. H.; Cacialli, F. Kelvin probe and ultraviolet photoemission measurements of indium tin oxide work function: a comparison. *Synth. Met.* **2000**, *111−112*, 311−314.
(31) Cambell, I. H.; Rubin, S.; Zawodzinski, T. A.; Kress, J. D.; Martin, R. L.; Smith, D. L.; Barashkov, N. N.; Ferraris, J. P. Controlling Schottky Energy Barriers in Organic Electronic Devices Using Self-assembled Monolayers. *Phys. Rev. B* **1996**, *54*, 14321−14314.
(32) Dupin, J.-C.; Gobeau, D.; Vinatier, P.; Levasseur, A. Systematic XPS Studies of Metal Oxides, Hydroxides and Peroxides. *Phys. Chem. Chem. Phys.* **2000**, *2*, 1319−1324.
(33) Beag, K.-J.; Bae, G.-T.; Noh, Y.-Y. Efficient Charge Injection in p-Type Polymer Field-Effect Transistors with Low-Cost Molybdenum Electrodes through V_2O_5 Interlayer. *ACS Appl. Mater. Interfaces* **2013**, *5*, 5804−5810.
(34) Yan, H.; Chen, Z.; Zheng, Y.; Newman, C.; Quinn, J. R.; Dötz, F.; Kastler, M.; Facchetti, A. A High-mobility Electron-transporting Polymer for Printed Transistors. *Nature* **2009**, *457*, 679−687.
(35) Caironi, M.; Newman, C.; Moore, J. R.; Natali, D.; Yan, H.; Facchetti, A.; Sirringhaus, H. Efficient Charge Injection from a High Work Function Metal in High Mobility N-type Polymer Field-effect Transistors. *Appl. Phys. Lett.* **2010**, *96*, 183303.
(36) Baeg, K.-J.; Khim, D.; Kim, D.-Y.; Jung, S.-W.; Koo, J. B.; You, I.-K.; Yan, H.; Facchetti, A.; Noh, Y.-Y. High Speeds Complementary Integrated Circuits Fabricated with All-Printed Polymeric Semiconductors. *J. Polym. Sci., Part B: Polym. Phys.* **2011**, *49*, 62−67.
(37) Luzio, A.; Criante, L.; D'Innocenzo, V.; Caironi, M. Control of Charge Transport in a Semiconducting Copolymer by Solvent-induced Long-range Order. *Sci. Rep.* **2013**, *3*, 3425.
(38) Kim, R.; Amegadze, P. S. K.; Kang, I.; Yun, H.-J.; Noh, Y.-Y.; Kwon, S.-K.; Kim, Y.-H. High-Mobility Air-Stable Naphthalene Diimide-Based Copolymer Containing Extended π-Conjugation for n-Channel Organic Field Effect Transistors. *Adv. Mater.* **2013**, *23*, 5719−5727.
(39) Park, J. H.; Jung, E. H.; Jung, J. W.; Jo, W. H. A Fluorinated Phenylene Unit as a Building Block for High-Performance n-Type Semiconducting Polymer. *Adv. Mater.* **2013**, *25*, 2583−2588.
(40) Kanimozhi, C.; Yaacobi-Gross, N.; Chou, K. W.; Amassian, A.; Anthopoulos, T. D.; Patil, S. Diketopyrrolopyrrole−Diketopyrrolopyrrole-Based Conjugated Copolymer for High-Mobility Organic Field-Effect Transistors. *J. Am. Chem. Soc.* **2012**, *134*, 16532−16535.
(41) Lv, A.; Puniredd, S. R.; Zhang, J.; Li, Z.; Zhu, H.; Jiang, W.; Dong, H.; He, Y.; Jiang, L.; Li, Y.; Pisula, W.; Meng, Q.; Hu, W.; Wang, Z. High Mobility, Air Stable, Organic Single Crystal Transistors of an n-Type Diperylene Bisimide. *Adv. Mater.* **2012**, *24*, 2626−2630.
(42) Liang, Z.; Tang, Q.; Xu, J.; Miao, Q. Soluble and Stable N -Heteropentacenes with High Field-Effect Mobility. *Adv. Mater.* **2011**, *23*, 1535−1539.
(43) Ortiz, R. P.; Herrera, H.; Blanco, R.; Huang, H.; Fecchetti, A.; Marks, T. J.; Zheng, Y.; Segura, H. L. Organic n-Channel Field-Effect Transistors Based on Arylenediimide-Thiophene Derivatives. *J. Am. Chem. Soc.* **2010**, *132*, 8840−8452.
(44) Zhang, F.; Hu, Y.; Schuettfort, T.; Di, C.-A.; Gao, X.; McNeill, C. R.; Thomsen, L.; Mannsfeld, S. C. B.; Yuan, W.; Sirringhaus, H.; Zhu, D. Critical Role of Alkyl Chain Branching of Organic Semiconductors in Enabling Solution-Processed N-Channel Organic Thin-Film Transistors with Mobility of up to 3.50 $cm^2 V^{-1} s^{-1}$. *J. Am. Chem. Soc.* **2013**, *135*, 2338−2349.
(45) Sun, B.; Hong, W.; Yan, Z.; Aziz, H.; Li, Y. Record High Electron Mobility of 6.3 $cm^2 V^{-1} s^{-1}$ Achieved for Polymer Semiconductors Using a New Building Block. *Adv. Mater.* **2014**, *26*, 2636−2642.
(46) Wei, Q.; Tajima, K.; Hashimoto, K. Bilayer Ambipolar Organic Thin-Film Transistors and Inverters Prepared by the Contact-Film-Transfer Method. *ACS Appl. Mater. Interfaces* **2009**, *9*, 1865−1868.
(47) Klauk, H.; Schmid, G.; Radlik, W.; Weber, W.; Zhou, L.; Sheraw, C. D.; Nichols, J. A.; Jackson, T. N. Contact Resistance in Organic Thin Film Transistors. *Solid-State Electron.* **2003**, *47*, 297−301.
(48) Xu, Y.; Gwoziecki, R.; Chartier, I.; Coppard, R.; Balestra, F.; Ghibaudo, G. Modified Transmission-line Method for Contact

Resistance Extraction in Organic Field-effect Transistors. *Appl. Phys. Lett.* **2010**, *97*, 063302.
(49) Baeg, K.-J.; Khim, D.; Jung, S.-W.; Kang, M.; You, I.-K.; Kim, D.-Y.; Facchetti, A.; Noh, Y.-Y. Remarkable Enhancement of Hole Transport in Top-Gated N-Type Polymer Field-Effect Transistors by a High-k Dielectric for Ambipolar Electronic Circuits. *Adv. Mater.* **2012**, *24*, 5433−5439.